Orthopositronium-sodium scattering using the close-coupling approximation in the integral representation

Prabal K. Sinha,[1] Puspitapallab Chaudhuri,[2] and A. S. Ghosh[3]
[1]*Department of Physics, Bangabasi College, 19, Raj Kumar Chakravorty Sarani, Calcutta 700 009, India*
[2]*Instituto de Fisica, Universidade de Sao Paulo, Caixa Postal 66318, 05315-970 Sao Paulo, Brazil*
[3]*Department of Theoretical Physics, Indian Association for the Cultivation of Science, Jadavpur, Calcutta 700 032, India*
(Received 28 June 2001; published 15 January 2002)

We investigate the scattering of orthopositronium by atomic sodium target at low and medium energies (up to 50 eV) using target-elastic and projectile-elastic close-coupling approximations (CCA) having different basis sets together with the static-exchange model. The low-energy elastic-scattering parameters are found to be consistent and the estimated binding energy for NaPs (in spin-singlet scattering) runs from 0.0042–0.0052 a.u. compared to value 0.005 892 a.u. obtained by using stochastic variational method [G. Ryzhikh and J. Mitroy, J. Phys. B **31**, L401 (1998)]. The elastic cross sections as obtained by different CCA models, except the static-exchange one, differ very marginally among themselves in the energy range 0.017–25 eV and 15 eV, onwards all the partial cross sections are very close to the corresponding exchange plane-wave estimates. At higher energies (above 15 eV), it is found that the major contribution to the total cross section comes from the positronium inelastic channels.

DOI: 10.1103/PhysRevA.65.022509 PACS number(s): 36.10.Dr, 34.50.−s

I. INTRODUCTION

Positronium (Ps) is a bound state of a particle (electron, e^-) and its antiparticle (position, e^+) and is available in two different spin states: the parapositronium (p-Ps) with antiparallel orientations of electron and positron spins having lifetime 125 ps while in ortho state (o-Ps) the parallel spin orientations results in a longer-lived state against the annihilation into gamma rays. The lifetime of o-Ps is approximately 10^3 times greater than that of p-Ps, consequently, o-Ps is more suitable for application purposes.

Due to the light mass and charge neutral character of Ps atom, it is suitable for being used as probe in different branches of science and technology [1]. For the analysis of the experimental data obtained with Ps as probe, it is essential to know how it interacts with individual atoms or molecules. None other than the scattering theory supplies the required information. Just about 15 years ago, the University College London (UCL) group has become capable of producing a stream of collimated Ps atoms, all having nearly the same energy [2] and their setup also allows us to change the energy value over a range (10–110 eV)—although the Ps beam available to date is not intense enough to perform the angular measurements in Ps projectile experiments. The total cross section has already been reported for different atomic (He, Ar) and molecular targets (H_2,O_2) [3–6]. Some experiments have also been performed to study the zero or near-zero energy cross sections, mainly for the atomic He target, using spectroscopic techniques [7–10].

Theoretically, Ps-atom/molecule scattering processes are much more complicated compared to a bare ion-atom/molecule scattering due to the bound structures of the projectile, as well as that of the target atoms and the appearance of multiparticle and multicenterd integrals in the exchange amplitudes [11]. As a result, until a few years ago, the progress in Ps projectile calculations was not very satisfactory, although pioneering work was performed by Massey and Mohr [12] as early as in 1954 using first-order exchange theory for the Ps-H system. In very recent times, due to the availability of high-speed computers, such calculations, using different forms of coupled-state representations, have gathered momentum [13]. In coupled-state formalism, the total wave function of the system is expanded in terms of the wave functions of bound subsystems. The effect of electron exchange, which is very important at low energies, is generally accounted for by antisymmetrizing the total wave function of the system.

Theoretically, Ps-H is the most extensively studied system, but no experiments to date have been performed on this system due to the difficulty of obtaining a nascent hydrogen target. Ps-He is the simplest system of this category in which the theoretical predictions can be judged in the background of experiments. There is a good deal of anomaly between the theories and measurements and also in between them for the low-energy cross section for Ps-He scattering. However, the *ab initio* coupled-state calculations for o-Ps-H/He systems conclusively indicate that at very low energies (near zero), the target inelastic channels affect the elastic parameters drastically [14–17] while with increasing energy, projectile inelastic channels become important [18–21]. It is to be noted that both H and He are much more strongly bound systems compared to the Ps atom.

Due to the discrepancies in the zero energy cross section of Ps-He scattering, it is quite natural to apply all the same attempts to other targets and observe the outcomes. For multielectron atoms, it is quite impossible to perform coupled-state calculations due to the complicacies in evaluating the exchange amplitudes. In contrary, the interaction dynamics of alkali atoms can easily be visualized by using a suitable quasi-one-electron picture due to their inert gas like core electronic structures. Due to this advantage and also keeping the desire of the UCL group [22] in mind, we plan to study the scattering of o-Ps atoms off atomic alkali targets at low

 ©2002 The American Physical Society

and medium energies using close-coupling approximations (CCA) taking sodium (Na) as an example. Another feature of Ps-alkali systems are that here both the colliding atoms have comparable binding energies, consequently, virtual target excitations are not expected to dominate the low-energy elastic scattering drastically over Ps excitation channels. Such studies can also focus light on the alkali-Ps bound structures; a few such bindings have already been reported theoretically by Ryzhikh and Mitroy using stochastic variational methods [23–25].

Considering these facts, we plan to study the scattering of o-Ps off an atomic sodium target at low and medium energies using different target-elastic and projectile-elastic CCA models [11]. Among the alkali atoms we choose Na for our present paper, as the UCL group will pursue measurements on Ps-Na scattering in the near future. In this paper, we visualize the target sodium atom as an effective one-electron atom and it is represented by the wave function of the valence electron. This is a reasonable approximation as $2p$ electrons of sodium are approximately nine times tightly bound compared to the valance electron. Different basis expansions will enable us to judge the relative importance of the added eigenstates in determining the scattering parameters. This dissertation reports the s-, p-, and d-wave scattering parameters along with the estimates for the zero-energy parameters and binding energies of sodium positride (NaPs). We also present an estimate for the total cross section for o-Ps-Na scattering up to incident energy 50 eV. At low energies (up to 25 eV), we employ the couple-state calculations and for higher energies, we use first-order theory. For describing the ground $(3s)$ and the excited $(3p,\ 4s,\ 3d,$ and $4p)$ states of the target Na atom, we use the orthonormalized wave functions due to Nielsen, Hansen, and Dubois, [26] who have used a frozen core-model potential to describe the quasi-one-electron Na atom as

$$V(r) = -\tfrac{1}{r}\{1 + (10 + 17.9635r)e^{-3.5927r}\}.$$

The validity of the wave functions at low energies is assured by the variational consistency of the scattering parameters. In the present paper, we use the following basis sets to study the system:

(a) $\mathrm{Ps}(1s) + \mathrm{Na}(3s)$,
(b) $\mathrm{Ps}(1s) + \mathrm{Na}(3s, 3p)$,
(c) $\mathrm{Ps}(1s) + \mathrm{Na}(3s, 3p, 4s)$,
(d) $\mathrm{Ps}(1s) + \mathrm{Na}(3s, 3p, 4s, 3d)$,
(e) $\mathrm{Ps}(1s) + \mathrm{Na}(3s, 3p, 4s, 3d, 4p)$,
(f) $\mathrm{Ps}(1s, 2s, 2p) + \mathrm{Na}(3s)$,
(g) $\mathrm{Ps}(1s, 2s, 2p, 3s, 3p, 3d) + \mathrm{Na}(3s)$.

The static-exchange model [model (a)] is the simplest among the coupled-state models as it incorporates only the ground states of the colliding atoms. The projectile-elastic CCA models [models (b)–(e)] include the excitation process(es) of the target atom keeping the projectile freezed in its ground state while the target-elastic CCA models [models (f) and (g)] account for the distortion of the projectile atom. We have not employed the full CCA model, which accounts for the simultaneous excitations of both the atoms. The present calculations are already very complicated and time consuming. Use of full CCA will increase the number of couple equations to $n = n_t \times n_p$, where n_t and n_p are the numbers of equations in projectile-elastic and the target-elastic CCA models, respectively. In this case, the number of matrix elements will be increased to a great extent and the evaluation of some of those (involving p and higher-angular momentum states) will involve multidimensional numerical integration.

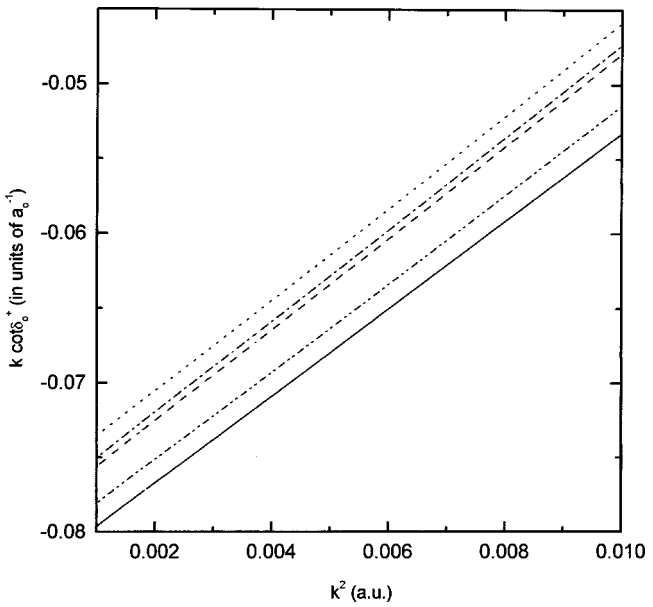

FIG. 1. Plot of $k \cot \delta_0^+$ vs k^2 for s-wave singlet scattering. Curves: dots, model (a); dash-dot, model (b); dash, model (e); dash-dot-dot, model (f); solid, model (g).

The theory for Ps-Na scattering is exactly same as Ps-H scattering and is described in detail in our earlier publications [15,18,27].

II. RESULTS AND DISCUSSIONS

We solve the one-dimensional coupled integral equations separately for the singlet- and triplet-scattering processes for individual partial waves starting from zeroth order to a maximum one, which depends on the incident energy. The maximum value of the partial wave up to which CCA calculations are performed, are so chosen that for at least the last two partial waves, the CCA and the Born give almost equivalent predictions. The contributions of the higher partial waves are replaced by the corresponding first-order estimates. For the proper evaluation of the exchange Born estimates (required as the inputs for CCA calculations) we use 28 gauss-Legendre points compared to 20 points required for Ps-H scattering. These extra points are required for the multiple nodes present in the Na states.

Figure 1 presents the $k \cot \delta_0^+$ (δ_0^+, is the s-wave singlet elastic phase shift in radian) plot against k^2 in the energy range $k = 0.01 - 0.1$ a.u. This figure contains the results of the static-exchange model and two projectile-elastic CCA models [models (b) and (e)] along with two target-elastic CCA models. Out of four projectile-elastic CCA models we

choose only two models (viz. b and e), as they will clearly indicate the effect of Na $(3p)$ state and the other excited states over Na $(3p)$. For estimating the zero-energy parameters, we extend our calculation down to $k=0.01$ a.u. and extrapolate the results to zero energy. It is evident from the figure that the inclusion of Na $(3p)$ state in the expansion scheme [model (b)] decreases the $k\cot\delta_0^+$ values moderately over those obtained in the static-exchange model [model (a)] while the other Na excitation channels have very marginal effect [model (e)]. That is, the rate of convergence of very low-energy *s*-wave singlet phase shifts is rather fast with the addition of target states in the expansion scheme. This is due to the fact that the lowest *p* state, here Na $(3p)$, accounts for most of the polarizabilities of the alkali atoms. In other words, through the addition of a Na $(3p)$ state, a significant portion of the target distortion is accounted for which is well reflected in the near-zero energy-scattering parameters. On the other hand, the projectile inelastic channels [models (f) and (g)] are found to have considerable influence on the near-zero energy *s*-wave singlet scattering parameters. Inclusion of Ps excitation channels reduces the $k\cot\delta_0^+$ values appreciably when compared with the corresponding values obtained by using static-exchange and the projectile-elastic CCA models. The difference between the models (f) and (g) are quite appreciable, i.e., other inelastic channels will influence the *s*-wave singlet scattering. In this connection, it is worth mentioning that for *o*-Ps-H and He elastic scattering near zero energy, it is found that the distortion of the tightly bound targets have a significant role over the comparatively loosely bound projectile inelastic channels, e.g., the near-zero energy cross sections (dominated by *s*-wave scattering) decrease drastically by the addition of the $n=2$ target inelastic channels. Here, projectile Ps is a relatively strongly bound system and its distortion affect the low-energy *s*-wave scattering more prominently than the target distortion. The *s*-wave singlet scattering length changes gradually form 12.9 a.u. in the static-exchange model to 12.7 a.u. in model (e), a change of 1.5%. On the other hand, the scattering length changes by about 7% in model (g) compared to the static-exchange prediction. The static-exchange model predicts the binding energy for the formation sodium positride (NaPs) to be 0.0042 a.u. which changes to 0.0044 a.u. in model (e), a model containing the maximum of the target excited states, the change being very marginal. On the other hand, our present target-elastic CCA model [model (g)] estimates the binding energy as 0.0052 a.u. Recently, Ryzhikh and Mitroy have employed the stochastic variational method [23] and obtained the value 0.005 892 a.u. for the NaPs binding. Our estimated values for the binding energy are in good agreement the value of Ryzhikh and Mitroy [23]. Clearly, a calculation including the effects of higher-excited states and continuum of the Ps atom is expected to give a higher magnitude for the binding energy.

The low-energy phase shift is a stringent test of models employed. In the absence of any experimental data, we test the merit of different models by comparing the values of the low-order (*s*, *p*, and *d* waves) and low-energy (up to energies below the first Na excitation threshold, which corresponds to the incident momentum $k=0.55$ a.u.) phase shifts. All the phase shifts are found to be variationally consistent, that is, with the addition of states in the basis set, the effective potential becomes more and more positive, which results in a higher values of the phase shifts.

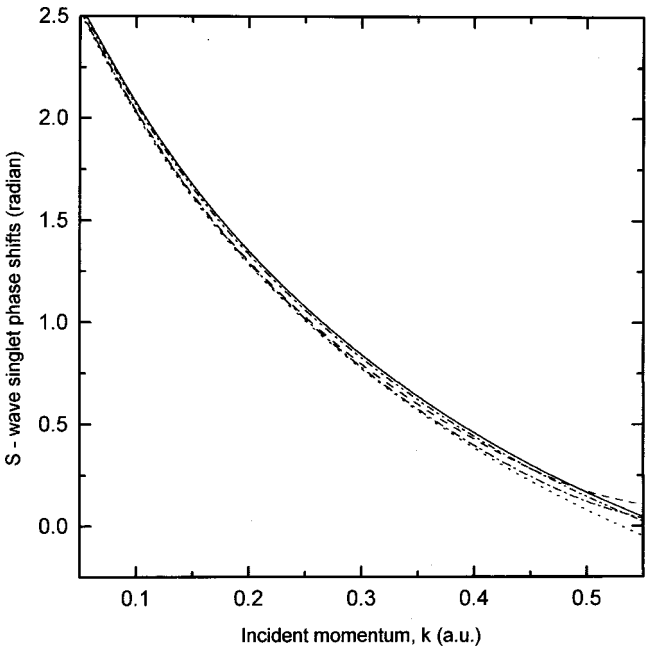

FIG. 2. *S*-wave singlet elastic phase shifts using different CCA models. Curves: dots, model (a); dash-dot, model (b); dash, model (e); dash-dot-dot, model (f); solid, model (g).

The *s*-wave singlet elastic phase shifts in the energy range $k=0.05-0.55$ a.u. are represented in Fig. 2 using the important five models (a, b, e, f, and g). All through this energy range, all the models predict almost the same values for phase shifts, the predictions of model (g) is the highest all around, while model (a) gives the least estimates. The virtual projectile inelastic channels affect the *s*-wave singlet scattering more than the virtual sodium inelastic channels. For triplet scattering (Fig. 3) the trend is the reverse. Here, the effect of target distortion increases the triplet phase shifts considerably and the effect increases with the increase in energy. At the highest energy shown in the figure, the triplet phase shifts changes from 0.938 in model (a) to 1.279 in model (b) and increases gradually with added target states in the expansion basis, to 1.349 in model (e). The difference between the triplet phase shifts obtained by using two target-elastic CCA models is very marginal all over the energy range considered. The other higher $(n>3)$ excited states of Ps atom is not expected to influence the triplet scattering significantly.

There is a recent report on Ps-Na [28] scattering using tuned model nonlocal exchange potential and observed resonances in the low-order phase shifts. It is this juncture we like to comment that CCA is a good method for resonance study at energies below the first excitation threshold of the scattering system. We have not encountered any resonance below the first Na excitation threshold and do not extend our calculation to above the threshold in search for resonance, as they may not be physical.

Figure 4 depicts the *p*-wave singlet phase shifts using different CCA models. Inclusion of the virtual excitation chan-

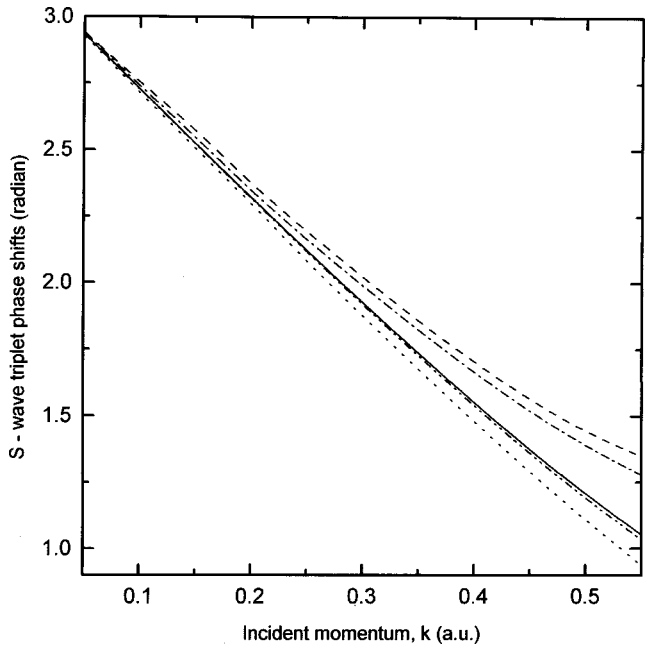

FIG. 3. *S*-wave triplet elastic phase shifts using different CCA models. Curves: dots, model (a); dash-dot, model (b); dash, model (e); dash-dot-dot, model (f); solid, model (g).

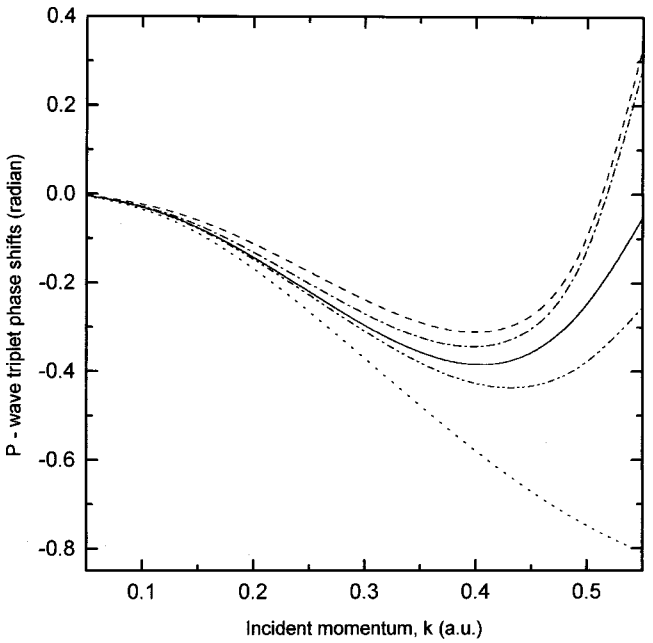

FIG. 5. *P*-wave triplet elastic phase shifts using different CCA models. Curves: dots, model (a); dash-dot, model (b); dash, model (e); dash-dot-dot, model (f); solid, model (g).

nel(s) of either atom in the basis set changes the *p*-wave phase shifts appreciably from the static-exchange predictions. Up to the incident energy $k=0.3$ a.u., the CCA models incorporating virtual target excitation channels [models (b) and (e)] give slightly higher values of phase shifts compared to those obtained by using models (f) and (g). In the energy range $k=0.3-0.55$ a.u., the projectile distortion effects influence the *p*-wave singlet scattering more than the target distortion effect. Just below the Na excitation threshold, the difference between the predictions of the CCA models are quite appreciable. At $k=0.55$ a.u., the inclusion of Ps $n=3$ states increases the phase shift from 0.6215 obtained with Ps $n=2$ states, to 0.6641. Thus, near threshold, higher excitation ($n>3$) and ionization channels is expected to influence *p*-wave singlet scattering. A moderate change is also observed in the predictions of models (b) and (e) at the highest energy. For *p*-wave triplet scattering (shown in Fig. 5), the virtual excitation channels of either atom have a significant affect and the influence increases with energy. Addition of the Na $(3p)$ channel in the basis set increases the triplet phase shifts appreciably at energies just below Na threshold. This phase shift is found to converge rapidly with the added Na states, as is evident from the marginal difference between the predictions of models (b) and (e). Whereas the convergence rate of the triplet phase shifts with the addition of Ps states is rather slow. Unlike *p*-wave singlet scattering, in triplet scattering, the projectile-elastic CCA models give higher values for the phase shifts all over the energy range under investigation, compared to those obtained by target-elastic models. All the models that include the polarization effects of the polarizable atom(s) show an upward trend in the triplet phase shift near the Na excitation threshold. All the calculations with Na excitation channels change the phase shift from negative values to the positive ones just below the threshold, i.e., target distortion effect(s) changes (change) the sign of the *p*-wave triplet potential.

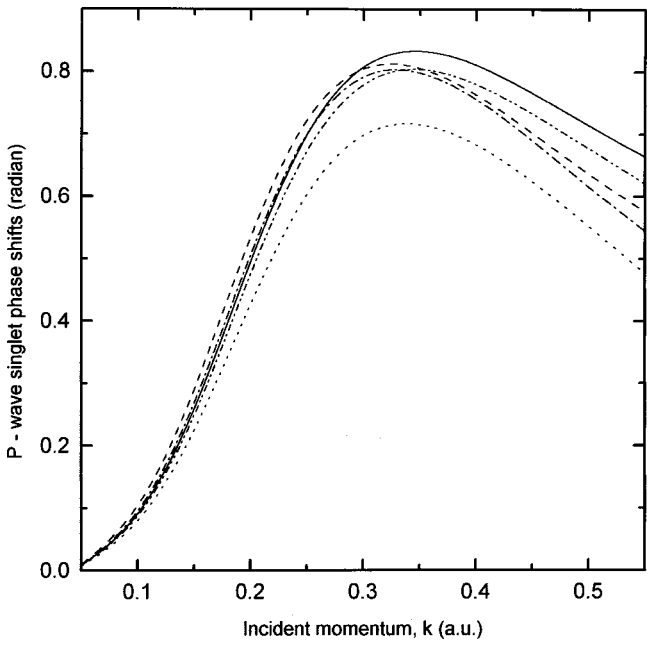

FIG. 4. *P*-wave singlet elastic phase shifts using different CCA models. Curves: dots, model (a); dash-dot, model (b); dash, model (e); dash-dot-dot, model (f); solid, model (g).

Figures 6 and 7 compare the *d*-wave elastic singlet and triplet phase shifts, respectively, using the different expansion basis within the framework of CCA. It is evident from the figures that the loss of target inelastic fluxes influence the *d*-wave elastic scattering more prominently than that caused by the Ps inelastic channels. For singlet scattering, Na $(3p)$

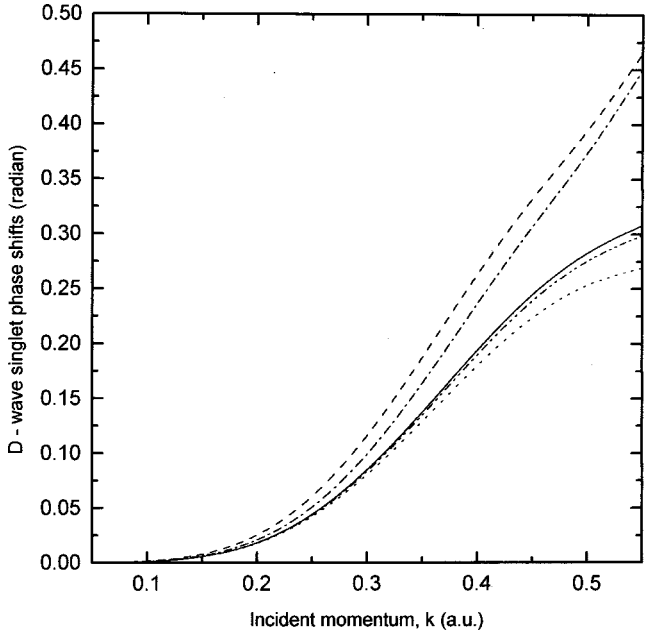

FIG. 6. *D*-wave singlet elastic phase shifts using different CCA models. Curves: dots, model (a); dash-dot, model (b); dash, model (e); dash-dot-dot, model (f); solid, model (g).

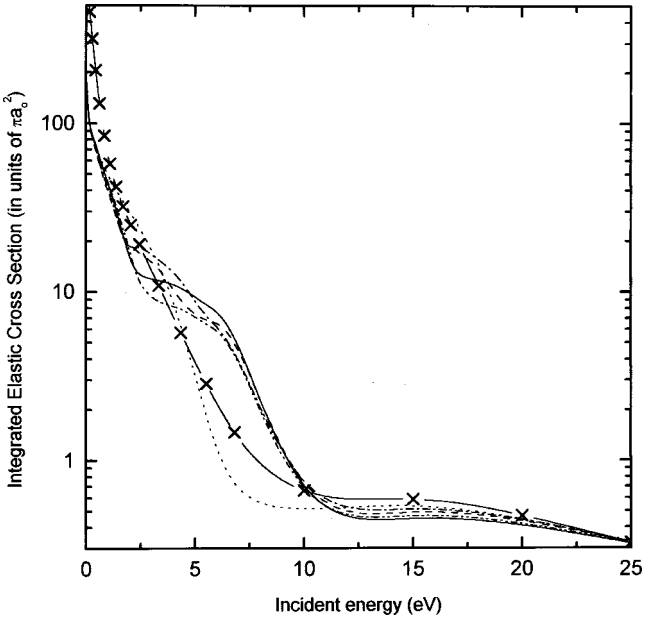

FIG. 8. Angle integrated elastic cross sections using different CCA models as well as first-order estimates. Curves: solid plus cross, the exchange FBA; dots, model (a); dash-dot, model (b); dash, model (e); dash-dot-dot, model (f); solid, model (g).

states produces the major change, while for triplet scattering, other higher-excitation channels do play a significant role. Inclusion of Ps $n=2$ states increase the phase shifts moderately, while $n=3$ states have a very marginal effect. Thus, for singlet *d*-wave scattering, the virtual excitation to Na $(3p)$ state causes the major change, while for triplet, other target inelastic channels have a notable effect.

Figure 8 compares the different estimates for the angle-integrated elastic cross sections obtained by employing the first-order exchange Born approximation (BO) as well as the other CCA models. As usual, at very low energies, the first-order theory over estimates the elastic cross section and gives a very large value ($721\pi a_0^2$ at 0.017 eV) while all the CCA models predict much lower values for the spin-averaged cross section [the corresponding values are 193, 181, 180, 177, and $174\pi a_0^2$ using models (a), (b), (e)–(g)]. It is interesting to note that near zero energy, cross sections do not change significantly by the inclusion of the target or the projectile inelastic channel(s). For Ps-H and He scattering at very low energies, it is found [14,17,27] that the $n=2$ excitation channels of the targets drastically reduce the cross section; the effect is more prominent for the He target than that for the H target. On the other hand, in both systems, the projectile inelastic channels (including excitations and ionization via pseudostates) reduce the elastic cross section very marginally [18,19,21,29]. It is interesting to note that in either case, the target is more tightly bound compared to the projectile atom. But in the present case, both the target and the projectile atoms have comparable binding energies and as a consequence, none of the virtual inelastic channels have a drastic effect on the low-energy elastic cross section. The cross section of model (a) falls rapidly compared to those of other CCA models, with an increase in energy. The maximum difference in the CCA cross sections, which incorporate the distortion effects of one of the colliding atoms, occurs around incident Ps energy 2 eV. With an increase in energy, all these estimates, together with that of model (a) converges towards the Born result, and 15 eV onwards, there is virtually no significant difference between all the six predictions contained in Fig. 8.

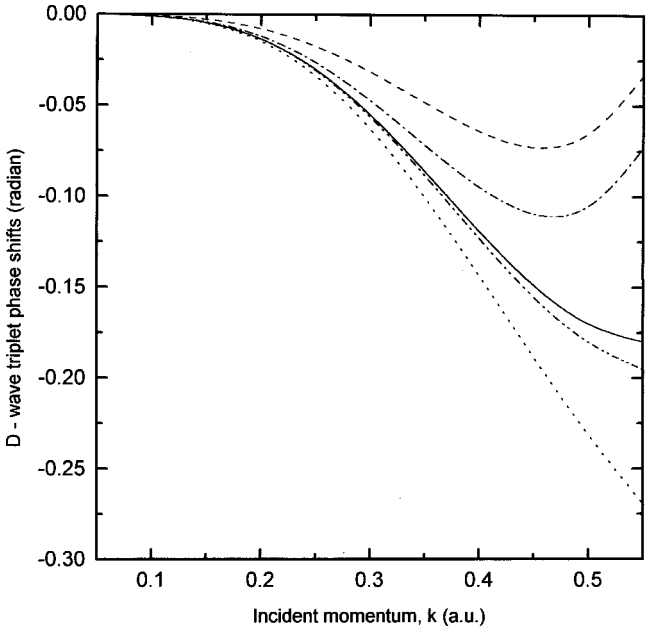

FIG. 7. *D*-wave triplet elastic phase shifts using different CCA models. Curves: dots, model (a); dash-dot, model (b); dash, model (e); dash-dot-dot, model (f); solid, model (g).

So far, inelastic cross sections (of target or projectile) are concerned it has been observed that 20 eV onwards, the FBA

with exchange gives fairly good estimates for the different angle-integrated partial cross sections. Thus, we execute the couple-state calculations up to 25 eV and for still higher energies, we rely on FBA exchange estimates. It is found for other targets that Ps ionization cross section contributes heavily to the total cross section for Ps-atom scattering at relatively high energies. So, we employed a nonexchange FBA model to calculate the Ps ionization cross section and found it to have a dominant contribution. This cross section grows 6.9 eV onwards to reach the peak at around 20 eV and falls quite slowly up to 50 eV. The total Na excitation [Na $(4s,\ 3p,\ 4p,$ and $3d)$] cross section as obtained by model (e) falls very rapidly up to 15 eV and then decreases steadily with energy. The total cross section of the system comprises of contributions coming from the elastic channel, the projectile inelastic (excitations and ionization) channels, and the target inelastic processes. All of these partial cross sections are added to the total cross section when they are energetically accessible. So, we define the present angle-integrated total cross section as

$$\sigma^T = \sigma^g_{\rm el} + \sigma^g_{{\rm Ps}(n=2,3)} + \sigma^{\rm BO}_{{\rm Ps}(n=4-6)} + \sigma^{\rm FBA}_{{\rm Ps}(ion)} + \sigma^e_{\rm Na}.$$

At energies below the first Na excitation threshold (2.108 eV), the elastic cross section is the only contributor to the total cross section, which falls with increasing energy. In estimating the total cross section, we use the results of model (g) for elastic contribution ($\sigma^g_{\rm el}$) as it has the most prominent effect on angle-integrated elastic cross sections. For Ps $n=2$ and 3 excitation contributions ($\sigma^g_{{\rm Ps}(n=2,3)}$), we use the values estimated by model (g) and Na excitation contributions ($\sigma^e_{\rm Na}$), the estimates of model (e) are employed up to incident Ps energy 25 eV. At still higher energies, first-order estimates have been used. Ps $n=4-6$ excitation cross sections ($\sigma^{\rm BO}_{{\rm Ps}(n=4-6)}$) are evaluated by exchange Born approximation and also for Ps ionization cross section ($\sigma^{\rm FBA}_{{\rm Ps}(ion)}$). Figure 9 displays the variation of the present total cross section (TCS) together with its components, with incident energy. The TCS shows two shallow picks; first, one is due to the opening of the Na excitation channel and the other is due to Ps excitation threshold. At medium energies (20–50 eV), the TCS is mainly comprised of the Ps inelastic cross sections, as the elastic and the Na excitation cross sections are very low.

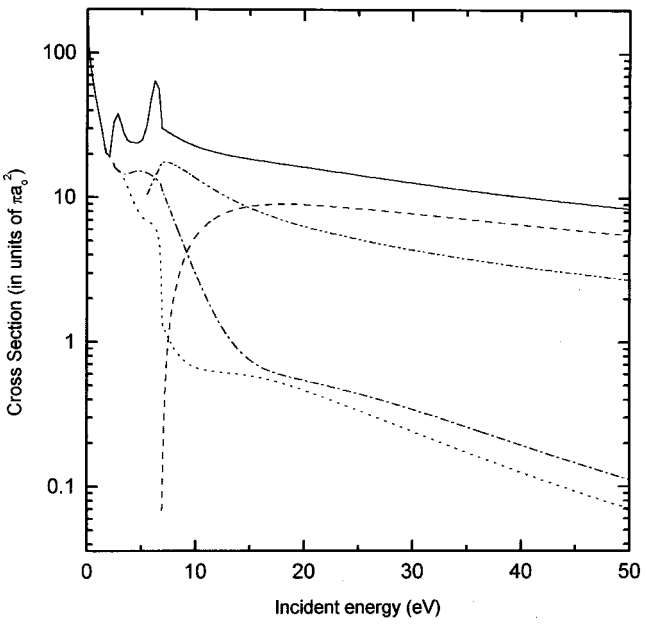

FIG. 9. Total cross section and its components for Ps-Na scattering. Curves: dot, elastic; dash, Ps ionization; dash-dot, Na excitations; dash-dot-dot, Ps excitations (up to $n=6$); solid, total cross section.

III. CONCLUSION

We investigate the scattering of Ps by sodium target at low and medium energies. Different target-elastic and projectile-elastic close-coupling models have been employed to study the system, in addition to the static-exchange model. In the target-elastic approximations, we use two different basis sets, whereas four projectile-elastic models have been used. This has been done to notice the effect of different inelastic fluxes of the atoms. We notice that our best target-elastic model [model (g)] influences the low-energy scattering parameters most significantly. The present results using projectile-elastic CCA models are found to be convergent with the addition of target eigenstates. All of the models employed in this paper, indicate the binding of NaPs in the spin-singlet case. Our best value for the binding energy is 0.0052 a.u., which is in good agreement with variational (stochastic) prediction 0.005 892 a.u. of Ryzhikh and Mitroy [23], their value being slightly higher. We also predict an estimate for the total cross section (addition of all partial cross sections) up to incident energy 50 eV. At low energies, the present elastic cross section differs significantly from the target-elastic CCA prediction of Adhikari and Mandal [28]. They have used a phenomenological tuned nonlocal potential to describe the exchange effect. Moreover, they have used a hydrogen $3s$ wave function with modified Bohr radius to describe the sodium ground state. This wave function does not include any effect of the core electrons. Our present models employed are *ab initio*, and theoretically sound and predicted results are expected to give good estimates. Moreover, including the same physics, the present method for H and He targets predict results, which are in good agreement with those of the Belfast group and those of Mitroy and his coworkers [30]. The present paper does not include the Ps ionization effect and the effect of simultaneous excitations of both of the atoms. Removal of these two restrictions may influence the low-energy elastic scattering. We advocate calculations including these two effects.

ACKNOWLEDGMENTS

The authors are thankful to the Department of Science and Technology, Government of India for financial support (SP/S2/K-31/96). One of us (P.C.) would like to thank Instituto de Fisica Teorica, Sao Paulo, Brazil for allowing us to use the computation facility of the Institute.

[1] D. M. Schrader, Nucl. Instrum. Methods Phys. Res. B **143**, 112 (1998).
[2] G. Laricchia, M. Charlton, S. A. Davies, C. D. Beling, and T. C. Griffith, J. Phys. B **20**, L99 (1987).
[3] N. Zafar, G. Laricchia, M. Charlton, and A. Garner, Phys. Rev. Lett. **76**, 1595 (1996).
[4] A. J. Garner, G. Laricchia, and A. Qzen, J. Phys. B **29**, 5961 (1996).
[5] A. J. Garner and G. Laricchia, Can. J. Phys. **74**, 518 (1996).
[6] A. J. Garner, A. Ozen, and G. Laricchia, Nucl. Instrum. Methods Phys. Res. B **143**, 155 (1998).
[7] Y. Nagashima, T. Hyodo, F. Fujiwara, and I. Ichimura, J. Phys. B **31**, 329 (1998).
[8] K. F. Canter, J. D. McNutt, and L. O. Roellig, Phys. Rev. A **12**, 375 (1975).
[9] P. G. Coleman, S. Rayner, F. M. Jacobsen, M. Charlton, and R. N. West, J. Phys. B **27**, 981 (1994).
[10] M. Skalsey, J. J. Engbrecht, R. K. Bithell, R. S. Vallery, and D. W. Gidley, Phys. Rev. Lett. **80**, 3727 (1998).
[11] A. S. Ghosh and P. K. Sinha, in *New Directions in Antimatter Chemistry and Physics*, edited by C. M. Surko and F. A. Gianturco (Kluwer Academic Publishers, Dordrecht, 2001).
[12] H. S. W. Massey and C. B. O. Mohr, Proc. Phys. Soc. London **67**, 695 (1954).
[13] A brief review of up-to-date works on Ps-atom scattering is available in Ref. [11].
[14] H. Ray and A. S. Ghosh, J. Phys. B **31**, 4427 (1998).
[15] A. Basu, P. K. Sinha, and A. S. Ghosh, Phys. Rev. A **63**, 012502 (2001).
[16] A. Basu, P. K. Sinha, and A. S. Ghosh, Phys. Rev. A **63**, 052503 (2001).
[17] A. S. Ghosh, A. Basu, T. Mukherjee, and P. K. Sinha, Phys. Rev. A **63**, 042706 (2001).
[18] P. K. Sinha, P. Chaudhuri, and A. S. Ghosh, J. Phys. B **30**, 4643 (1997).
[19] C. P. Campbell, M. T. McAlinden, F. G. R. S. McDonald, and H. R. J. Walters, Phys. Rev. Lett. **80**, 5097 (1999).
[20] N. K. Sarkar and A. S. Ghosh, J. Phys. B **30**, 4591 (1997).
[21] J. E. Blackwood, C. P. Campbell, M. T. McAlinden, and H. R. J. Walters, Phys. Rev. A **60**, 4454 (1999).
[22] G. Laricchia (private communication with A. S. Ghosh).
[23] G. Ryzhikh and J. Mitroy, J. Phys. B **31**, L401 (1998).
[24] J. Mitroy and G. Ryzhikh, J. Phys. B **32**, 3839 (1999).
[25] J. Mitroy and G. G. Ryzhikh, Comput. Phys. Commun. **123**, 103 (1999).
[26] S. E. Nielsen, J. P. Hansen, and A. Dubois, J. Phys. B **28**, 5295 (1995).
[27] P. K. Sinha, A. Basu, and A. S. Ghosh, J. Phys. B **33**, 2579 (2001).
[28] S. K. Adhikari and P. Mandal, J. Phys. B **34**, 1361 (2001).
[29] N. K. Sarkar, P. Chaudhuri, and A. S. Ghosh, J. Phys. B **32**, 1657 (1999).
[30] J. Mitroy (private communications with A. S. Ghosh).